



## Fabrication of three-dimensional microfluidic channels in glass by femtosecond pulses

Cunxia Li, Xu Shi, Jinhai Si\*, Tao Chen, Feng Chen, Ai Qin Li, Xun Hou

Key Laboratory for Physical Electronics and Devices of the Ministry of Education, Shanxi Key Lab of Information Photonic Technique, School of Electronics and Information Engineering, Xi'an Jiaotong University, Xianing-xilu 28, Xi'an, Shanxi 710049, China

### ARTICLE INFO

#### Article history:

Received 25 September 2008

Received in revised form 13 October 2008

Accepted 30 October 2008

### ABSTRACT

Fabrication of three-dimensional microfluidic channels in glasses by water-assisted ablation with femtosecond laser pulses was investigated. The experimental results showed that formation of the photoinduced microchannels by femtosecond pulses depended on the incident laser power and the scanning speed. For the same scanning speed, the shape of cross-section of channels changed from ellipse to circle with increasing the laser power. Under the optimum condition of laser processing, we fabricated two layers of microfluidic channels with diameter of about 8  $\mu\text{m}$  inside glass. The distance between two layers of microchannels was about 20  $\mu\text{m}$ .

Crown Copyright © 2008 Published by Elsevier B.V. All rights reserved.

### 1. Introduction

Microfluidic components including microcell, microchannels and micropump can be applied in a variety of fields such as biochemical analysis, medical inspection, new drug development, and environment monitoring [1]. Commonly, microchannels are achieved by UV lithography [2], wet etching [3] and then the bonding technology [4]. Although these techniques have been well established, these methods are tedious to form three-dimensional (3D) microstructures. With the rapid development of ultrashort-pulse technology, femtosecond laser pulses provide a unique micromachining tool that allows the surface or bulk of a transparent material to be modified with micrometer precision. A tightly focused femtosecond laser pulse can deposit energy into a transparent material through high-order nonlinear absorption, producing 3D-localized material ablation either on the surface or in the bulk. Femtosecond laser direct writing is suitable for rapid prototyping. Therefore, many researchers have paid much attention to the fabrication of microfluidic components with femtosecond laser pulses.

Marcinkevicius et al. demonstrated femtosecond laser-assisted 3D microstructure of H-shaped channel in silica glass that was carried out in two steps: writing a preprogrammed pattern to the silica volume by using laser pulses to produce uniformly distributed damage spots and then etching the glass in a 5% aqueous solution of HF acid [5]. Masuda et al. produced 3D microstructures such as microcells and microchannels inside the photosensitive glass by focused femtosecond laser pulses irradiation, followed by chemical etching with a HF acid solution of modified regions [6]. In 2001, Li

et al. have drilled micro-holes from the rear surface of silica glass in contact with distilled water [7]. When distilled water was introduced into the hole, the effects of blocking and redeposition of ablated material were greatly reduced and the aspect ratio of the depth of the hole was increased. No postfabrication such as heat treatment or wet etching is needed, nor are toxic chemicals used. Furthermore, the method avoids multiples bonding steps that are heavily utilized in planar microfabrication. Using this method, many researches have been carried out to fabricate different microstructures in recent years [8–11]. To date until now, however, there are very few reports on the fabrication of multilayers microchannels inside glass or other materials.

In this paper, we present our experimental results of microfluidic channels fabricated in glass by water-assisted ablation with femtosecond laser pulses. The experimental results showed that formation of the photoinduced microchannels by femtosecond pulses depended on the incident laser power and the scanning speed. In the processing procedure, we first fabricated a microchannel that was perpendicular to the glass surface by focusing the laser beam onto the rear surface of the glass, which was in contact with distilled water. After water flows into the channel due to the capillary phenomenon, we fabricated two layers of microchannels by moving the focal spot along the horizontal direction.

### 2. Experimental setup

Fig. 1 shows the schematic diagram of the experimental system for the laser microfabrication. A regeneratively amplified Ti:sapphire laser system was used, which delivered pulses with duration of 30 fs (FWHM), center wavelength at 800 nm and repetition rate of 1 kHz. The laser beam was focused onto the glass sample by a microscope objective. The energy of the incident pulses could be

\* Corresponding author.

E-mail address: [jinhaisi@mail.xjtu.edu.cn](mailto:jinhaisi@mail.xjtu.edu.cn) (J. Si).

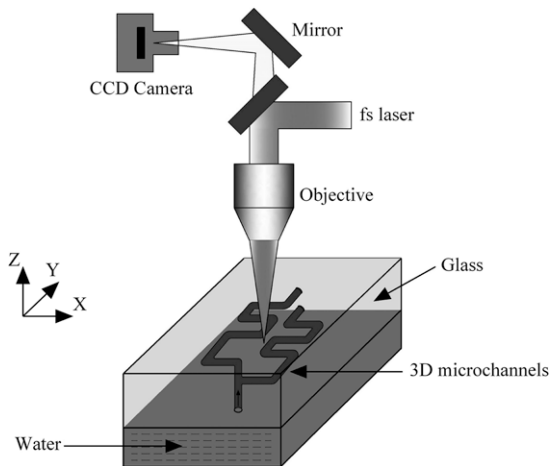


Fig. 1. Schematic setup for fabrication of a 3D microfluidic channels.

continuously varied by a variable attenuator. A mechanical shutter was employed to select the appropriate ablation time. The glass sample with a thickness of 0.6 mm was mounted on a computer controlled 3D translation stage with a resolution of 0.04  $\mu\text{m}$ .

We first focused the laser beam on the rear surface of the glass sample that was in contact with distilled water by the microscope objective ( $20\times$ ,  $\text{NA} = 0.45$ ) and translated the glass along the  $z$  direction step by step as shown in Fig. 1. By scanning the focal point at constant speed towards the front surface, a channel was fabricated. After that, the sample was moved in the  $xy$  plane to form other hollow microchannels. The images were captured by the CCD camera.

### 3. Results and discussion

By varying the power of the incident beam and the scanning speed, we investigated the influence of pulse energy and scanning speed on processing quality. We first made a straight channel about 40  $\mu\text{m}$  length in the vertical direction by moving the sample along the  $z$  direction, where the average power of the incident beam was kept at 10  $\mu\text{W}$ , and then translated the sample along the  $y$  direction to fabricate the hollow channels. Fig. 2 shows the dependence of the maximum length of the photoinduced microchannels on the laser average power when the scanning speed was kept at 0.5  $\mu\text{m}/\text{s}$ . From Fig. 2, we can see that the maximum

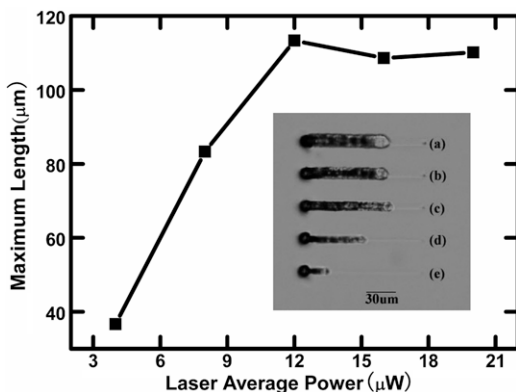


Fig. 2. Dependence of the maximum length of the photoinduced microchannels on the laser average power when the scanning speed was kept at 0.5  $\mu\text{m}/\text{s}$ . The inset shows the fabricated microchannels, where laser average power was set at (a) 20  $\mu\text{W}$ , (b) 16  $\mu\text{W}$ , (c) 12  $\mu\text{W}$ , (d) 8  $\mu\text{W}$  and (e) 4  $\mu\text{W}$ , respectively.

length of the photoinduced channel increased with the increase of the laser power, and when laser power was increased to 12  $\mu\text{W}$ , the length of channels didn't increase any longer. In addition, we can see that the higher laser power was, the larger diameter of the channels was. Therefore, high pulse energy was disadvantageous to fabricate the high quality channels. We also investigated the dependence of the maximum length of the photoinduced microchannels on the scanning speed when the laser average power was kept at 5  $\mu\text{W}$ . The results are shown in Fig. 3, from which we can see that a longer channel was able to be fabricated at a slower scanning speed. If the scanning speed was too rapid, the dust and ablated debris have no enough time to disperse in water, so a block was formed in the channels and impeded removal of the plume. In addition, we found that these channels have the same width, and it didn't depend on the scanning speed. Therefore, slow scanning speed was favorable for fabricating long channels. In a word, pulse energy and scanning speed had distinct influence on the processing quality.

Note the inset of Figs. 2 and 3, the thick black area was channels formed under the fabrication condition described above, while the thin white line was not but filamentous damage track induced by the femtosecond laser. In the channel processing, accompanied by the inflow of water, the channel could elongate continuously. Once the ablated debris could not eject effectively, the length of the channels no longer increased and the filamentous damage track occurred rather than channels.

In addition, we have observed the shape of cross-section of the channels. The scanning way of the channels was the same as the above experiments. The cross-section was perpendicular to the  $y$  direction. In general, the cross-sectional profile of the fabricated microchannels showed an elliptical shape [12,13]. For instance, a cross-section is shown in Fig. 4a, where laser power was set at 10  $\mu\text{W}$  and scanning speed was 0.5  $\mu\text{m}/\text{s}$ . When the laser power was increased from 10  $\mu\text{W}$  to 35  $\mu\text{W}$ , however, the shape of cross-section of the channels became from ellipse to circle, as shown in Fig. 4. With the increase of the laser power, the aspect ratio of the microchannel cross-section increased, and the cross-sectional shape of the microchannels became into circle from ellipse. This is probably because ablated materials in the channels confined the penetrative depth of the laser pulses. When the power was increased, the diameter of the channels increased, which made the ablated materials easily flow out from the channels. Therefore, laser pulses penetrated further into the glass and ablated more glass in the laser propagation direction.

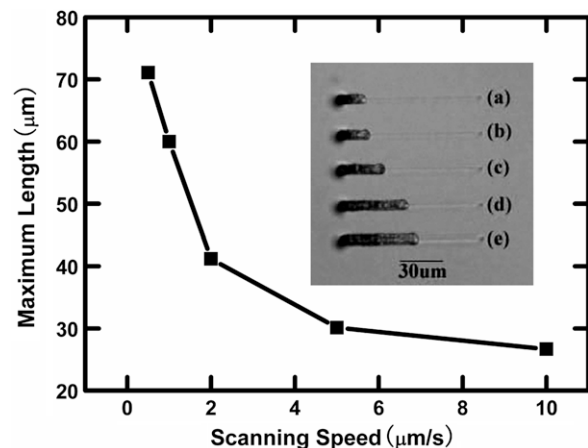


Fig. 3. Dependence of the maximum length of the photoinduced microchannels on the scanning speed when the laser average power was kept at 5  $\mu\text{W}$ . The inset shows the fabricated microchannels, where the scanning speed was set at (a) 10  $\mu\text{m}/\text{s}$ , (b) 5  $\mu\text{m}/\text{s}$ , (c) 2  $\mu\text{m}/\text{s}$ , (d) 1  $\mu\text{m}/\text{s}$  and (e) 0.5  $\mu\text{m}/\text{s}$ , respectively.

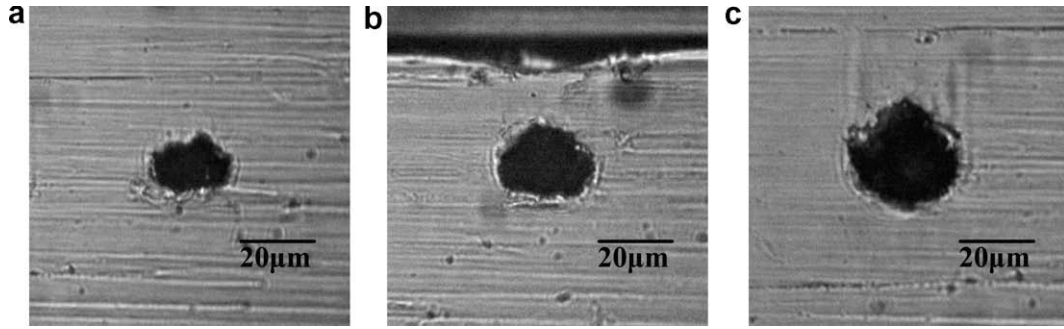


Fig. 4. The images of cross-section of the photoinduced microchannels for different laser powers: (a) 10  $\mu\text{W}$ , (b) 25  $\mu\text{W}$  and (c) 35  $\mu\text{W}$ .

To confirm the fabricated microchannels in the glass were hollow structures, we observed the fabricated E-shaped microstructures for two cases: (a), the microstructures filled with water, and (b), the microstructures without water. From Fig. 5, we can see that the microstructures filled with water and the microstructures without water showed bright and dark patterns, respectively.

In the fabrication process, the ablation debris ejection and efficient dispersion into water were critical. Therefore, choosing appropriate laser energy and scanning speed were required to fabricate 3D microchannels. According to the experimental results described above, the laser average power and the scanning speed

were set at 5  $\mu\text{W}$  and 0.2  $\mu\text{m/s}$ , respectively. As shown in Fig. 6a, we first translated the sample along the z direction to fabricate the channel. Accompanied by the inflow of water, the channel elongated continuously. When the channel reached a length of 50  $\mu\text{m}$ , we closed shutter and moved the sample in the opposite direction to the 30  $\mu\text{m}$  length position. After the distilled water flowed into the channel and dispersed the debris of the sample, we translated the sample along the x and y direction to fabricate the square wave-shaped microchannel. Next, we moved the sample and fabricated another symmetrical microchannel in the second layer. The distance between the first layer and the second

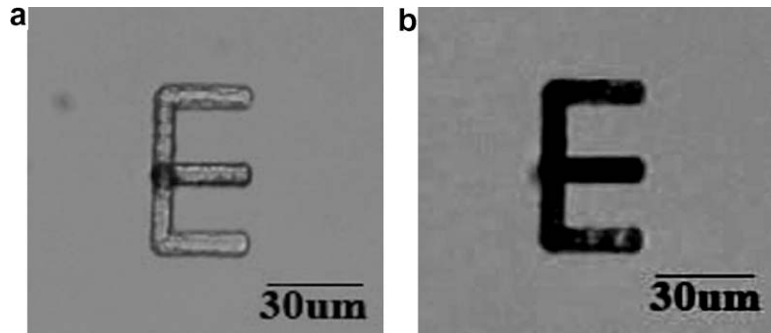


Fig. 5. Top view of the fabricated E-shaped microstructures inside the glass: (a) filled with water and (b) unfilled with water.

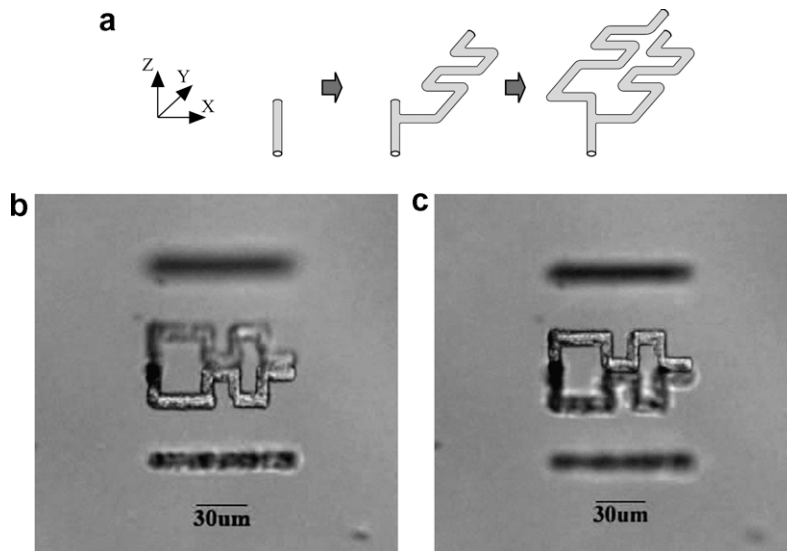


Fig. 6. Procedure and microscopic photographs of a 3D microchannels fabricated in the glass by femtosecond pulses: (a) the procedure for fabricating the 3D microchannels. Microscopic photographs of the fabricated microchannels on the first layer (b) and the second layer (c) inside the glass.

layer was about 20  $\mu\text{m}$ . During the machining process of microchannels, the dust and debris dispersed in the water and flowed out of the hole constantly, so the true hollow channels could be fabricated. Fig. 6b and c show two microscopic photographs of the 3D microchannels. We could see clearly that two layers of microchannels filled with water were fabricated inside the glass. The diameter of microchannels was about 8  $\mu\text{m}$ . In order to show the fabricated microchannels were inside the glass, we ablated two grooves on the front and the rear surface, respectively.

#### 4. Conclusion

In summary, we investigated the fabrication of 3D microfluidic channels inside glass by water-assisted ablation with femtosecond laser pulses. Two layers of microchannels with diameter of about 8  $\mu\text{m}$  were fabricated in the glass sample. It is expected that this technique will be applied to the fabrication of 3D microfluidic components including microcell, microchannels and micropump.

#### Acknowledgements

The authors gratefully acknowledge the financial support for this work provided by the National Science Foundation of China

under the Grant Nos. 10674107 and 60678011, and the National Key Scientific Research Foundation of China under the Grant No. 2006CB921602.

#### References

- [1] Y. Iga, W. Watanabe, T. Ishizuka, Y. Li, J. Nishii, K. Itoh, Proc. SPIE 5062 (2003) 129.
- [2] X. Liu, D. Du, G. Mourou, IEEE J. Quant. Electron. 33 (1997) 1706.
- [3] C. Hnatovsky, R.S. Taylor, E. Simova, P.P. Rajeev, D.M. Rayner, V.R. Bhardwaj, P.B. Corkum, Appl. Phys. A 84 (2006) 47.
- [4] L. Martynova, L.E. Locascio, M. Gaitan, G.W. Kramer, R.G. Christensen, W.A. Maccreehan, Anal. Chem. 69 (1997) 4783.
- [5] A. Marcinkevicius, S. Juodkazis, M. Watanabe, M. Miwa, S. Matsuo, H. Misawa, J. Nishii, Opt. Lett. 26 (2001) 277.
- [6] M. Masuda, K. Sugioka, Y. Cheng, N. Aoki, M. Kawachi, K. Shihoyama, K. Toyoda, H. Helvajian, K. Midorikawa, Appl. Phys. A 76 (2003) 857.
- [7] Y. Li, K. Itoh, W. Watanabe, K. Yamada, D. Kuroda, J. Nishii, Y.Y. Jiang, Opt. Lett. 26 (2001) 1912.
- [8] R. An, Y. Li, Y. Dou, Y. Fang, H. Yang, Q. Gong, Chin. Phys. Lett. 21 (2004) 2465.
- [9] D.J. Hwang, T.Y. Choi, C.P. Grigoropoulos, Appl. Phys. A 79 (2004) 605.
- [10] R. An, Y. Li, Y. Dou, H. Yang, Q. Gong, Opt. Express 13 (2005) 1855.
- [11] R. An, Y. Li, Y. Dou, D. Liu, H. Yang, Q. Gong, Appl. Phys. A 83 (2006) 27.
- [12] Y. Cheng, K. Sugioka, K. Midorikawa, M. Masuda, K. Toyoda, M. Kawachi, K. Shihoyama, Opt. Lett. 28 (2003) 55.
- [13] R. Osellame, S. Taccheo, M. Marangoni, R. Ramponi, P. Laporta, D. Polli, S. De Silvestri, G. Cerullo, J. Opt. Soc. Am. B 20 (2003) 1559.